White Rose Research Online

eprints@whiterose.ac.uk
https://eprints.whiterose.ac.uk
Universities of Leeds, Sheffield and York

Deposited via The University of Sheffield.

White Rose Research Online URL for this paper:
https://eprints.whiterose.ac.uk/id/eprint/209033/

Version: Accepted Version

Article:
Singh, R., O'Farrell, T., Biagi, M. et al. (2023) Vector coding optical wireless links. Journal of Lightwave Technology, 41 (17). pp. 5577-5587. ISSN: 0733-8724

https://doi.org/10.1109/jlt.2023.3265628

© 2023 The Authors. Except as otherwise noted, this author-accepted version of a journal article published in Journal of Lightwave Technology is made available via the University of Sheffield Research Publications and Copyright Policy under the terms of the Creative Commons Attribution 4.0 International License (CC-BY 4.0), which permits unrestricted use, distribution and reproduction in any medium, provided the original work is properly cited. To view a copy of this licence, visit http://creativecommons.org/licenses/by/4.0/

Reuse
This article is distributed under the terms of the Creative Commons Attribution (CC BY) licence. This licence allows you to distribute, remix, tweak, and build upon the work, even commercially, as long as you credit the authors for the original work. More information and the full terms of the licence here: https://creativecommons.org/licenses/

Takedown
If you consider content in White Rose Research Online to be in breach of UK law, please notify us by emailing eprints@whiterose.ac.uk including the URL of the record and the reason for the withdrawal request.

UNIVERSITY OF LEEDS
University of Sheffield
UNIVERSITY of York

Vector Coding Optical Wireless Links

Ravinder Singh, Timothy O'Farrell, Mauro Biagi, Richard, V. Penty, and John P. R. David

***Abstract*—The quasi-static nature of the optical wireless channel means that the channel state information (CSI) can be readily available at the transmitter and receiver prior to data transmission. This implies that electrically band-limited optical wireless communication (OWC) systems can make use of optimal channel partitioning or vector coding based multi-channel modulation (MCM) to achieve high throughput by mitigating the non-linearities arising from the optical and electrical channel. This paper proposes a pulse amplitude modulation (PAM) based DC-biased optical vector coding (DCO-VC) MCM scheme for OWC. The throughput performance of DCO-VC is evaluated and compared to the well known DC-biased optical orthogonal frequency division multiplexing (DCO-OFDM) over hybrid (line-of-sight and diffuse) and diffuse (non line-of-sight only) visible light communication (VLC) channels with additive white Gaussian noise. For the completeness of the VLC physical layer, the performance comparison is based on an uncoded and a forward error correction transmission mode using well-known convolutional codes with Viterbi decoder. The results show that the coded DCO-VC outperforms DCO-OFDM system by achieving up to 2 and 3 dB signal to noise ratio gains over hybrid and diffuse VLC channels, respectively.**

***Index Terms*—Optical wireless communication, Visible light communication, OFDM, Vector coding, Rate-adaptive channel coding, Multi-channel modulation.**

I. Introduction

RISING numbers of smart interconnected devices, bandwidth hungry computer applications transferring data between machines and limited RF spectrum have resulted in the research, development and standardisation of VLC systems [1][2]. Simultaneously, providing high-speed wireless communication and lighting through a single source, with lower carbon footprint solid-state lighting devices [3] has further motivated research in VLC systems globally. Unregulated spectrum, high data rates and cost effective system front ends are some of the other advantages of VLC [4]–[6]. VLC systems use intensity modulation (IM) and direct detection (DD), where the transmitter and receiver are generally realised by light emitting diode(s) (LEDs) and photo detector(s) (PDs), respectively. Use of advanced multiple-input multiple-output (MIMO) [7][8] and multi-colour [9]–[11] VLC systems as well as hybrid VLC-RF networks [12][13] have been proposed to avoid a predicted capacity crunch on the wireless channel in the near future [14].

VLC, which has been mainly proposed for indoor wireless communication, suffers from multipath dispersion (or inter-symbol interference, ISI) as multiple copies of a transmitted pulse are present at the receiver due to reflections from indoor objects and walls [15] as well as due to the slow response of the opto-electronic devices involved [16]–[18]. Multi-channel (multi-carrier) modulation (MCM) schemes have been widely deployed in wired and wireless communication networks due to their ability to combat moderate to severe ISI.

The conventional MCM schemes cannot be used directly in IM/DD links as the transmit signal has to be real and unipolar. Therefore, to overcome dispersion, various optical MCM schemes based on OFDM and discrete multi-tone (DMT) have been developed for VLC such as DCO-OFDM [19][20], asymmetrically clipped optical OFDM (ACO-OFDM) [21], Unipolar OFDM (U-OFDM) [22], Flip-OFDM [23] and PAM-DMT [24], which provide a real and non-negative transmit signal. PAM based single-channel modulation (SCM) with frequency domain equalisation (FDE) has also been proposed as a low peak-to-average power ratio (PAPR) alternative [25][26]. When compared with coherent complex systems, the non-DC-biased MCM systems sacrifice at least one-half of the system capacity to attain real and unipolar transmit signal. In the case of DC-biased systems, they increase power requirements to attain a real and unipolar transmit signal modulating the intensity of LEDs [27]. Therefore, the overall throughput of the VLC systems is limited by the front-end electrical bandwidth and the type of signalling sets that can be used in the IM/DD system.

Given all the power and spectral inefficiencies related to the above mentioned VLC signalling schemes, there is a need for a new signalling scheme that is specifically designed to meet the channel conditions imposed and has the ability to make efficient use of the known CSI at the transmitter. Keeping this in mind, we propose the use of optimal channel partitioning vectors (or vector coding) for the design of a new MCM scheme for VLC systems. The vector coding (VC) scheme can partition the known VLC channel into orthogonal sub-channels to transmit data in parallel [28][29]. This matches with the quasi-static nature of the VLC channel, where the CSI is readily available to the communicating points. The proposed DC-biased optical vector coding (DCO-VC) scheme uses M-PAM modulation over each sub-channel with a DC-bias to provide a real and unipolar electrical signal which modulates the intensity of the LED source(s).

The DCO-OFDM offers higher bit-rate, for a certain BER, to the bandwidth-limited VLC systems when compared to the non-DC-biased OFDM schemes, such as ACO-OFDM, U-

R. Singh was with the Centre for Photonic Systems, Department of Engineering, University of Cambridge, Cambridge, UK, CB3 0FA. Most of this work formed part of the PhD thesis of Ravinder Singh completed in 2016 at the University of Sheffield, UK. He is currently with Toshiba Europe Ltd., Cambridge Research Laboratory, Cambridge CB4 0GZ, UK. (e-mail: rsingh@crl.toshiba.co.uk)

M. Biagi is with the Department of Information, Electrical and Telecommunication (DIET) engineering, "Sapienza" University of Rome, Via Eudossiana 18, 00184, Italy. (e-mail: mauro.biagi@uniroma1.it)

R. V. Penty is with the Centre for Photonic Systems, Department of Engineering, University of Cambridge, Cambridge, UK, CB3 0FA (e-mail: rvp11@cam.ac.uk).

T. O'Farrell and J. P. R. David are with the Department of Electronic and Electrical Engineering, University of Sheffield, Sheffield S1 3JD, United Kingdom (e-mail: {t.ofarrell, j.p.david}@shef.ac.uk,)

OFDM [30][27]. Therefore, this paper focuses on the DC-biased MCM schemes and evaluates the throughput performance of uncoded and coded DCO-OFDM and DCO-VC systems using representative hybrid (line-of-sight and diffuse) and diffuse only (non line-of-sight) channels with AWGN. Our investigations show that the proposed DCO-VC system outperforms the DCO-OFDM scheme in both the uncoded and coded transmission modes. In the hybrid channels, the coded DCO-VC system provides up to 2 dB signal to noise ratio (SNR) gain in comparison to the coded DCO-OFDM. Over the diffuse channels, the DCO-VC system achieves up to 1 and 3 dB SNR gain in uncoded and coded modes, respectively, when compared to the DCO-OFDM counterparts for the same throughput. The throughput results over hybrid and diffuse indoor VLC channels also show that as the dispersion increases the SNR gains of the DCO-VC system improve further.

The rest of the paper is organised in the following manner. Section III presents the wireless VLC channel used in this paper. Section II details the basis and working of the DCO-VC and DCO-OFDM systems. The throughput performance evaluation for an AWGN channel is presented in section IV, where the analytical model for throughput evaluation is also presented. Section V presents the throughput performance results over the hybrid and diffuse VLC channels. Finally, section VI gives the concluding remarks.

Notations: In this paper, lower-case bold fonts represent a vector and upper-case bold fonts represent a matrix. Q is the Q-function, $(.)^T$ represents vector transpose, and $(.)^H$ denotes Hermitian transpose.

II. Description of MCM schemes studied

This section details the basis of DCO-OFDM and DCO-VC MCM schemes investigated in this paper in uncoded and coded transmission modes.

A. Coded DCO-OFDM MCM

Fig. 1 shows a schematic diagram of a coded DCO-OFDM system. At the Tx, random binary data (r) is encoded through forward error correction (FEC) coding (see section II-C for details) and grouped into $k = \log_2(M)$ bits for baseband modulation, generally M-QAM. Here M is the modulation order. The modulated data symbols (z_i) are then divided into $N/2$ parallel sub-channels in the frequency-domain (FD), where N is the FFT size (and the total number of sub-channels). This is done to satisfy the Hermitian symmetry constraint in the FD, so that a real bipolar signal can be obtained in the time-domain (TD). Therefore, each FD DCO-OFDM symbol, $\mathbf{z} = [z_0, z_1, \ldots, z_{N-1}]^T$ must satisfy:

$$\begin{cases} z_0 = z_{\frac{N}{2}} = 0, & \text{DC Subcarrier} \\ z_{(\frac{N}{2}-L)} = z^H_{(\frac{N}{2}+L)}, & L = 1, 2, \ldots, \frac{N}{2} - 1 \end{cases} \quad (1)$$

where, $(\cdot)^H$ denotes Hermitian transpose and z_i is a complex M-QAM symbol. The bipolar TD DCO-OFDM symbol $\mathbf{x}$ is then obtained after IFFT of FD symbol $\mathbf{z}$. A cyclic prefix (CP) of length μ, which is a copy of the last μ elements of $\mathbf{x}$, is then added to avoid ISI between OFDM symbols at the cost of reduced data rate. The real, bipolar continuous TD signal $x_b(t)$ is then obtained after parallel to serial conversion and digital to analogue conversion (DAC). A DC-bias (B_{dc}) is added then to ensure non-negativity and signal $x_u(t)$ is obtained which modulates the intensity of the LED(s). Details about the B_{dc} set-up can be found in section II-E.

At the Rx, post DD, the received signal $y(t)$ can be given as:

$$y(t) = TR(x(t) * h(t)) + n(t), \quad (2)$$

where, "$*$" denotes the convolution operator, T is the transmissivity of the optical filter, R is the responsivity (A/W) of the PD, $h(t)$ represents the impulse response of the wireless VLC channel and $n(t)$ represents the AWGN with a constant variance of $\sigma^2 = N_o/2$, where N_o is the single-sided noise power spectral density and has units of W/Hz.

Each received DCO-OFDM symbol, after analogue to digital conversion (ADC), is represented by $\mathbf{y}$. After CP removal, the Fourier transform of the received symbol $\mathbf{y}$ gives back the FD OFDM symbol $\tilde{\mathbf{z}}$ and then the FD zero-forcing equalisation (FD-ZFE) takes place. Each received DCO-OFDM symbol undergoes equalisation to obtain the i^{th} equalised sub-carrier $\hat{z}_i = \tilde{z}_i/h_i$ such that $\hat{\mathbf{z}} = \tilde{\mathbf{z}}/\mathbf{h}$, where $\mathbf{h}$ is the length N frequency response vector of the VLC channel. The baseband demodulation in terms of hard-decision (HD) or soft-decision (SD) detection (see section II-D) and Viterbi decoding are then performed on $\hat{\mathbf{z}}$ to retrieve final information bits. The minimum mean square error (MMSE) can be used as an alternative equalisation technique. However, given the VLC channels are not highly frequency selective, relatively less complex zero-forcing equalisation (ZFE) has been found to provide MMSE equivalent performance [25].

B. Concept of proposed coded DCO-VC

Vector coding (VC) is known as the optimal channel partitioning MCM technique [29]. Since the indoor VLC channel is mostly quasi-static in nature[1], CSI will be readily available at the transmitting end. This is ideally matched to the requirement of VC. VC uses singular value decomposition (SVD) of the circulant channel matrix $\mathbf{H}_{N\times(N+\mu)}$, where N is the number of sub-channels and μ is the CP length. For a finite impulse response (FIR) h_n, $0 \leq n \leq \mu-1$, of a discrete-time channel, the circulant channel matrix can be written as [29][31]:

$$\mathbf{H} = \begin{bmatrix} h_0 & h_1 & \ldots & h_{\mu-1} & 0 & \ldots & 0 \\ 0 & h_0 & \ldots & h_{\mu-2} & h_{\mu-1} & \ldots & 0 \\ \vdots & \vdots & \ddots & \ddots & \ddots & \ddots & \vdots \\ 0 & \ldots & 0 & h_0 & \ldots & h_{\mu-2} & h_{\mu-1} \end{bmatrix} \quad (3)$$

The SVD of the above matrix $\mathbf{H}$ can be given as:

$$\mathbf{H} = \mathbf{USV}^H, \quad (4)$$

where, $\mathbf{U}_{N\times N}$ and $\mathbf{V}_{(N+\mu)\times(N+\mu)}$ are two unitary matrices. $\mathbf{S}_{N\times(N+\mu)}$ is a diagonal matrix which contains singular values

[1]Except for the special use cases where the user terminal is rapidly moving around, such as a robot.

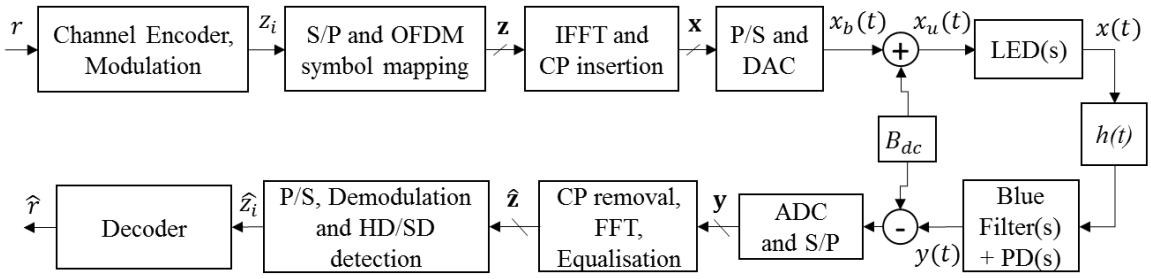

Fig. 1. Transceiver block diagram of DCO-OFDM MCM with FEC.

(s_i) of $\mathbf{H}$ on its diagonal elements [29][31]. VC uses matrix $\mathbf{V}$ at the transmitter for precoding to create N parallel independent sub-channels. The rows of matrix $\mathbf{U}$ are used as discrete time matched filters at the receiver.

Fig. 2 shows the schematic of a DCO-VC system with FEC. After the channel encoding, baseband modulation takes place. In this work, an M-PAM modulation scheme has been used in order to obtain a real and bipolar vector precoded signal. The PAM symbols are grouped into vectors of length N, known as a DCO-VC symbol vector. Each DCO-VC symbol vector[2] can be represented as $\mathbf{z} = [z_0, z_1, \ldots, z_{N-1}]^T$ and the precoded data vector $\mathbf{x}$ is obtained from $\mathbf{z}$ as $\mathbf{x} = \mathbf{V}\mathbf{z}$. As the size of $\mathbf{V}$ is $(N+\mu) \times (N+\mu)$, in order for the precoding to take place either μ zeros are appended at the end of each DCO-VC symbol vector or the original DCO-VC vector of length N is processed by the first N columns of $\mathbf{V}$ [29]. Each precoded vector can be given as $\mathbf{x} = [x_0, x_1, \ldots, x_{N+\mu-1}]^T$ and also includes a prefix of length μ. The precoded vectors represent a real bipolar DCO-VC signal which undergoes DAC and the continuous time signal $x_b(t)$ is obtained to which B_{dc} (see section II-E) is added to obtain the real unipolar VC signal, $x_u(t)$. The transmitted and received signals in DCO-VC can also be given by $x(t)$ and $y(t)$, hence, (2) applies.

At the Rx, after B_{dc} removal by subtraction and ADC, each DCO-VC vector can be mathematically represented as:

$$\mathbf{y} = \mathbf{H}\mathbf{x} + \mathbf{n} \tag{5}$$

In equation (5), $\mathbf{n}$ represents an AWGN vector, each element having a standard deviation of σ_n. Equation (5) can be rewritten as $\mathbf{y} = \mathbf{U}\mathbf{S}\mathbf{V}^H\mathbf{V}\mathbf{x}+\mathbf{n}$. Then the prefix is removed and the matched filter operation at the receiver takes place which can be represented as:

$$\mathbf{U}^H\mathbf{y} = \mathbf{U}^H\mathbf{U}\mathbf{S}\mathbf{V}^H\mathbf{V}\mathbf{x} + \mathbf{U}^H\mathbf{n} \tag{6}$$

By rewriting (6), the filtered vectors at Rx can be represented as $\tilde{\mathbf{z}} = \mathbf{S}\mathbf{x} + \mathbf{U}^H\mathbf{n}$, where $\tilde{\mathbf{z}} = \mathbf{U}^H\mathbf{y}$ and $\mathbf{U}^H\mathbf{n}$ has unchanged noise variance, since $\mathbf{U}$ is a unitary matrix. Equivalent zero-forcing equalisation in DCO-VC is realised by dividing each received sub-channel $\tilde{z}_i$ by s_i, which gives $\hat{z}_i$ and hence $\hat{\mathbf{z}}$. This is not an optimal way to equalise because sub-channel gains less than 1 enhance the noise in that sub-channel. However, this was done to provide a fair comparison between the considered schemes. An optimal way to detect a signal in DCO-VC , which is a part of further investigation to the authors, would be to adjust the detector threshold in the PAM demodulator according to known $\mathbf{S}$ at the Rx. Once $\hat{\mathbf{z}}$ is obtained, the HD or SD detection takes place as detailed in section II-D and final information bits are obtained through Viterbi decoding.

[2]Unlike DCO-OFDM, in DCO-VC $\mathbf{z}$ contains real, bipolar sub-channels.

C. Encoder and Modulation set-up

The HD and SD detection based DCO-OFDM and DCO-VC systems used a 64 state binary convolutional (BC) code with the well-known industry standard generator polynomials: $\{171,133\}$ and code rates 1/2, 2/3 and 3/4 through puncturing patterns specified in [32]. Six different modulation modes for each signalling scheme were considered; 2, 4, 8, 16, 32 and 64 PAM for DCO-VC and 4, 16, 64, 256, 1024 and 4096 QAM for the DCO-OFDM system. This was done to keep the spectral efficiency (or bits/sub-channel) the same for all the considered systems, e.g. 64-PAM based DCO-VC and 4096-QAM based DCO-OFDM will result in approximately the same bits/sub-channel due to the Hermitian symmetry requirement of DCO-OFDM.

D. Hard and soft information de-mappers

In HD detection, the i^{th} M-PAM or M-QAM received symbol, $\widehat{z}_i$, is detected from the i^{th} sub-channel (or element) of $\hat{\mathbf{z}}$ as:

$$\widehat{z}_i = \underset{\alpha \in \mathcal{A}}{\operatorname{argmin}} |\hat{z}_i - \alpha|^2, \tag{7}$$

where, $\mathcal{A}$ is the set gathering baseband modulation alphabet. The final coded data bits are then de-mapped from $\widehat{z}_i$ and are forwarded to the channel decoder to retrieve the information bits $\widehat{r}$.

In the case of SD detection, the log-likelihood ratios (LLRs) of each received binary bit are acquired from the i^{th} sub-channel $\hat{z}_i$. This can be done through either a maximum *a posteriori* probability (MAP) algorithm or by an approximate LLR computation algorithm. The MAP based LLR algorithm computes the LLR of the q^{th} binary bit (r_i^q), for $0 \leq q \leq k-1$, from the i^{th} received sub-channel $\hat{z}_i$ as [33]:

$$\mathcal{L}(r_i^q) = \frac{1}{N_o}\left\{ \min_{\alpha \in \mathcal{A}^{q=0}} |\hat{z}_i - \alpha|^2 - \min_{\alpha \in \mathcal{A}^{q=1}} |\hat{z}_i - \alpha|^2 \right\}, \tag{8}$$

where, $\mathcal{A}^{q=1}$ and $\mathcal{A}^{q=0}$ are the subsets of the baseband modulation constellation alphabet, and represent an alphabet with q^{th} bit labelled as '1' and '0', respectively.

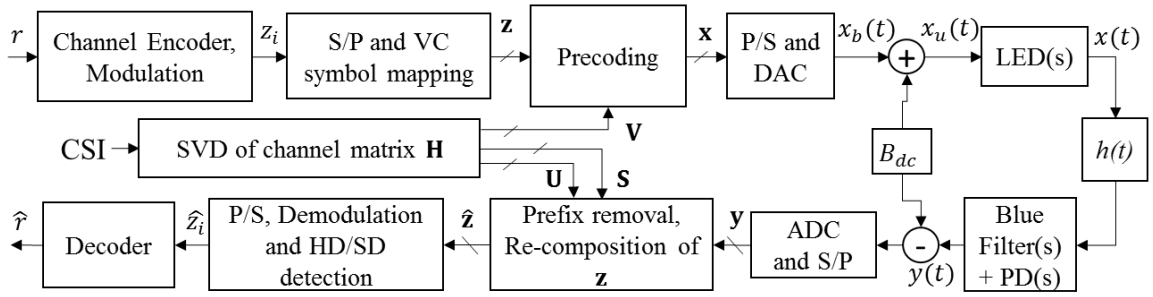

Fig. 2. Transceiver block diagram of DCO-VC MCM with FEC.

In our investigation, however, an approximate LLR computation method detailed in [34] was used due to the high computational complexity of the MAP based LLR algorithm. As an example, for 8-PAM modulation in DCO-VC, the LLR of b_i^q from $\hat{z}_i$ can be obtained as [34]:

$$\mathcal{L}(b_i^q) = \begin{cases} \hat{z}_i, & q=0 \\ |\hat{z}_i| - 4, & q=1 \\ \left.\begin{array}{l} 2-|\hat{z}_i|, \text{ for } |\hat{z}_i| \le 4 \\ |\hat{z}_n| - i, \text{ for } |\hat{z}_i| > 4 \end{array}\right\}, & q=2 \end{cases} \tag{9}$$

These approximate LLRs are then forwarded to the decoder to obtain the decoded binary information stream. The approximate LLR algorithm in (9) can also be applied separately to the in-phase and quadrature components of a 64-QAM based $\hat{z}_i$ in DCO-OFDM to obtain the total of 6 soft bits. This approximate LLR detection is also known as the threshold detection technique. In a similar manner, the approximate LLRs for different M level modulations were obtained.

E. The DC-bias (B_{dc})

In the considered modulation schemes, B_{dc} was set based on the mean electrical power of $x_b(t)$, as in the literature [21][35], which can be given as:

$$B_{dc} = \kappa\sqrt{E\{x_b^2(t)\}}, \tag{10}$$

where κ is a constant of proportionality and $E\{\cdot\}$ is the expectation operator. In dB, the B_{dc} is given as $10\log_{10}(\kappa^2) + 10\log_{10}(E\{x_b^2(t)\})$. Any negative sample(s), that are left after adding B_{dc} are clipped to zero, so that a clipped unipolar signal $x_u(t)$ can be obtained:

$$x_u(t) = x_b(t) + B_{dc} + n_{clip}(t), \tag{11}$$

where $n_{clip}(t)$ is the additive clipping distortion with power or variance $\sigma^2_{n_{clip}}$.

In this paper, for the considered optical signalling schemes B_{dc} was set to keep $n_{clip}(t)$ negligible, such that a target BER of 10^{-6} can be achieved and the irreducible BER floor due to clipping is set substantially below the target BER. Fig. 3 shows the B_{dc} values used in this paper, for a certain spectral efficiency with DCO-VC and DCO-OFDM schemes, to achieve the target BER. This way, the considered systems were investigated without any dynamic range constraints at Tx.

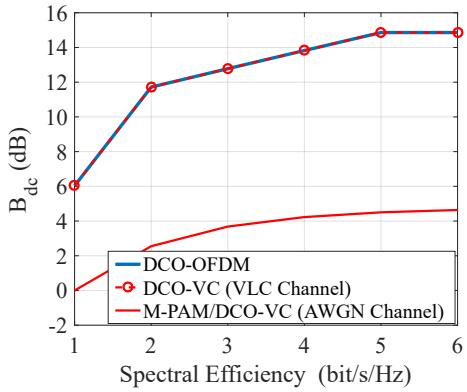

Fig. 3. B_{dc} values used for considered uncoded and coded optical signalling schemes to achieve target BER of 10^{-6}.

It can be seen from Fig. 3 that the DCO-VC system has the same B_{dc} requirements as DCO-OFDM system for a VLC channel. It is worth remarking that, for an AWGN channel the DCO-VC system reduces to an equivalent DC-biased M-PAM system. For an AWGN channel, the channel matrix $\mathbf{H}$ contains ones on its diagonal elements and SVD of such a matrix gives identity $\mathbf{U}$, $\mathbf{S}$ and $\mathbf{V}^H$ matrices. Therefore, precoding and matched filtering operations do not change the transmit and receive signals, respectively. This means $\mathbf{x} = \mathbf{z}$, which contains M-PAM modulated symbols. Therefore, in an AWGN channel the B_{dc} requirements of DCO-VC are very low and are equivalent to those of a DC-biased M-PAM system. This is not the case for a VLC channel, were the decomposition of $\mathbf{H}$ provide different $\mathbf{S}$ and $\mathbf{V}^H$ matrices which change the nature of the transmit signal.

III. The Wireless VLC Channel

A typical indoor office environment is shown in Fig. 4 with a transmitter (Tx) situated at ceiling height and a receiver (Rx) at desk level height [24][36]. The indoor wireless VLC channel between Tx and Rx is composed of a line-of-sight (LOS) path and multiple delayed paths reflected off the walls, ceiling, floor and other indoor objects [37]. The channel impulse response (CIR) of such a hybrid channel containing LOS and multiple reflected paths can be modelled as [24]:

$$h(t) = \eta\delta(t - \Delta t_{LOS}) + \frac{\zeta}{\tau_c}\exp\left(-\frac{t - \Delta t_{Dif}}{\tau_c}\right)u(t - \Delta t_{Dif}), \tag{12}$$

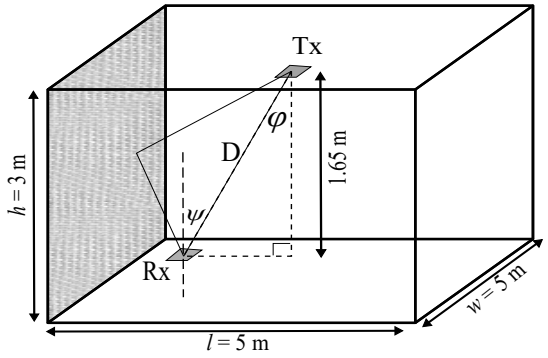

Fig. 4. VLC system setup in a typical indoor office environment.

where τ_c is the time-constant of the exponentially decaying diffuse channel; Δt_{LOS} and Δt_{Dif} are the signal delays of the LOS and diffuse paths ($\Delta t_{Dif} \geq \Delta t_{LOS}$), respectively; η and ζ are the LOS and diffuse channel gains, respectively, and are given as:

$$\eta = \begin{cases} \frac{(m+1)A}{2\pi D^2} \cos^m(\phi) \cos(\psi) g_c(\psi), & \psi < \Psi \\ 0, & \psi > \Psi \end{cases} \tag{13}$$

$$\zeta = \frac{A}{A_{Room}} \frac{\rho}{(1-\rho)} \tag{14}$$

In (13), m is the Lambertian emission order, given as $-\log_2[\cos(\phi_{\frac{1}{2}})]$, where $\phi_{\frac{1}{2}}$ is the LED's semi-angle at half-power. D is the physical distance between the Tx and Rx, A is the surface area of the detector, $g_c(\psi)$ is the optical concentrator gain, ϕ is the angle of irradiance, ψ is the angle of incidence and Ψ is the field-of-view (FOV) of the PD. In (14), A_{Room} is the room surface area which can be calculated as:

$$A_{Room} = 2(l \cdot w + l \cdot h + w \cdot h), \tag{15}$$

and ρ is the average reflectivity of the room surfaces. In (15) l, h and w are the length, height and width of the room, respectively. In this paper, the considered VLC systems have been investigated without the use of an optical concentrator, therefore, $g_c(\psi)$ is unity. All the system parameters are listed in Table I. The ϕ and ψ can be calculated from the orientation and physical location of the Tx and Rx in the model room.

The τ_c in (12) can be calculated as [38]:

$$\tau_c = -\frac{\langle t \rangle}{\ln(\rho)}, \tag{16}$$

where $\langle t \rangle$ is the mean time between two reflections which can be approximated as (17)[38], where c is the speed of light.

$$\langle t \rangle = \frac{4(l \cdot w \cdot h)}{cA_{Room}} \tag{17}$$

IV. System Performance over AWGN Channels

This section details the throughput performance of the uncoded and coded, DCO-VC and DCO-OFDM systems examined over an AWGN channel through simulations and analytical approximations to verify the accuracy of system models.

TABLE I
VLC System Parameters.

Parameter	Value
A	10 mm^2
A_{Room}	110 m^2
$g_c(\psi)$	1
FOV, Ψ	70°
LED semiangle at half power, $\phi_{\frac{1}{2}}$	60°
Optical Filter Transmissivity, T [39]	0.7
PD Responsivity, R [40]	0.4 A/W
LED and Filter Central Wavelength (λ_c)	450 nm
System Bandwidth (W)	20 MHz

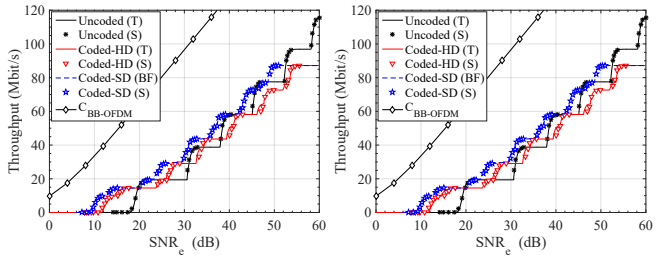

Fig. 5. Throughput of uncoded and coded (HD and SD) a) DCO-VC and b) DCO-OFDM over AWGN channel. (T) and (S) in the legends signifies the theoretical and simulation results, respectively. The dashed line shows the best-fit (BF) throughput curve obtained by curve fitting from the simulations for SD.

A. System Throughput

The throughput of the DCO-VC and DCO-OFDM systems can be estimated through (18) and (19), respectively, where Γ is the code rate and P_{SR} is the packet success rate given as $P_{SR} = (1 - \text{BER})^{\ell}$, where ℓ is the packet length in bits and BER is achievale bit error rate by the uncoded, coded-HD and coded-SD configurations of each system. Packets with 1500 data bytes were transmitted and system bandwidth W of 20 MHz was considered during all the simulations in this paper. This bandwidth is sufficiently lower than many commercial sources and detectors and therefore, the simulations assume no non-linearities arising due to the electrical channel. The ISI in the considered systems arise due to the limited bandwidth of the optical channel. The presented throughput curves are optimised by selecting the most energy efficient combination of Γ and M.

$$\mathcal{T}_{\text{DCO-VC}} = W\left(\frac{N}{N+\mu}\right)\Gamma \log_2(M) P_{SR}, \tag{18}$$

$$\mathcal{T}_{\text{DCO-OFDM}} = W\left(\frac{N/2-1}{N+\mu}\right)\Gamma \log_2(M) P_{SR}, \tag{19}$$

The results in Fig. 5a and Fig. 5b in general show that the Coded-SD scheme is the most energy efficient over the majority of the electrical SNR (SNR$_e$) scale. The Coded-HD scheme can provide some gain at low SNR$_e$. However, as SNR$_e$ increases above 30 and 36 dB in DCO-VC and DCO-OFDM systems, respectively, the Coded-HD schemes yield no gain and perform worse than the higher order uncoded schemes. On the other hand for both the DCO-VC and DCO-OFDM, the Coded-SD schemes, provide an SNR$_e$ gain of

up to 9 dB in comparison to uncoded schemes and up to 5 dB gain when compared to Coded-HD schemes. In addition to reduction in the SNR gains of Coded-HD schemes with increasing SNR_e, it can be noticed that the gains with Coded-SD schemes are also reduced. This is due to the well-known decrease in coding gain with increasing modulation order in BC coded systems. Furthermore, a coded system with a certain Γ, must work with a high M scheme to achieve a high throughput and will require higher B_{dc} leading to reduced energy efficiency. This combined effect leads to the throughput of coded systems to be worse than the uncoded systems.

B. Shannon Capacity

Fig. 5a and Fig. 5b, also show the Shannon capacity curves for the real bipolar-baseband (BB) configuration of the considered systems, i.e. in the electrical domain where the detection takes place. The BB configuration for capacity estimation was used as a reference, which indicates the additional power penalty due to B_{dc} requirements in VLC systems that reduce the attainable throughput for a certain SNR. The channel sum capacity of the BB-VC and BB-OFDM systems can be estimated as:

$$C_{\text{BB-VC}} = \frac{W}{2(N+\mu)} \sum_{i=0}^{N-1} \log_2(1+\text{SNR}_\text{e}(i)), \tag{20}$$

$$C_{\text{BB-OFDM}} = \frac{W}{(N+\mu)} \sum_{i=1}^{\frac{N}{2}-1} \log_2(1+\text{SNR}_\text{e}(i)), \tag{21}$$

respectively. In (20) and (21), $\text{SNR}_\text{e}(i)$ is the electrical SNR in the i^{th} sub-channel or sub-carrier and can be given as:

$$\text{SNR}_\text{e}(i) = \frac{T^2R^2|h_i|^2P_i^2}{\sigma^2}, \tag{22}$$

where, P_i^2 is the average electrical transmit power of the i^{th} sub-channel with transmitted optical power P_i and σ^2 is the electrical noise power at the receiver.

C. Analytical throughput estimation

The analytical throughput results for the uncoded and Coded-HD MCM systems are also presented in Fig. 5a and Fig. 5b, respectively. Such analytical estimates are not readily available for the SD detection. In order to obtain these analytical results, the BERs of DCO-VC and DCO-OFDM systems were first estimated theoretically, which were then converted to throughput using (18) and (19). In the following sequel, the analytical models used for the BER performance estimation are detailed.

1) Uncoded bit error probability: The bit error probability of the PAM based DCO-VC systems over the AWGN channel can be estimated through the union bound as:

$$\mathcal{P}_{b(\text{DCO-VC})} \leq \frac{1}{Mlog_2(M)} \sum_{i=1}^{M} \sum_{\substack{j=1,\\ j\neq i}}^{M} Q\left(\sqrt{\frac{d(s_i,s_j)^2}{4\sigma_n^2}}\right), \tag{23}$$

where, $d(s_i, s_j)$ is the Euclidean distance between two legitimate M-PAM symbols in signal space with added B_{dc} and $Q(\cdot)$ is the tail probability of the standard normal distribution. The bit error proability of the QAM based OFDM systems can be estimated as [41]:

$$\mathcal{P}_{b(\text{DCO-OFDM})} = \frac{2(\sqrt{M}-1)}{\sqrt{M}\log_2(\sqrt{M})} Q\left(\sqrt{\frac{3P^2}{(M-1)\sigma_n^2}}\right) + \frac{2(\sqrt{M}-2)}{\sqrt{M}\log_2(\sqrt{M})} Q\left(3\sqrt{\frac{3P^2}{(M-1)\sigma_n^2}}\right), \tag{24}$$

where, P^2 is the average transmitted electrical power of the DCO-OFDM signal for optical power P, and is given as $P^2 = (\kappa^2+1)$. It must be noted that high B_{dc} values used during simulations to achieve the target BER results in negligible $n_{clip}(t)$, which can be omitted for the evaluation of the analytical bit error probabilities. For lower B_{dc} values, (23) and (24) must be modified taking n_{clip} into account.

2) Coded-HD throughput: The bit error probability for the Coded-HD schemes can be estimated analytically as [42][43]:

$$\mathcal{P}_{b(\text{Coded-HD})} = \frac{1}{\log_2(M)} \sum_{w=d_{free}}^{d_{free}+N_{st}} \beta_w \mathcal{P}_w, \tag{25}$$

where w is an index representing the Hamming weight between the transmitted and received codeword, d_{free} is the free distance of the convolutional code, N_{st} is the number of significant codewords, β_w is the total number of bit errors corresponding to all the weight w codewords which are tabulated in [44][45], and $\mathcal{P}_w$ is the error probability of selecting an incorrect trellis path (or codeword) of weight difference w given as [46]:

$$\mathcal{P}_w = \begin{cases} \sum\limits_{j=\lceil w/2 \rceil}^{w} \binom{w}{j} \mathcal{P}_b^j (1-\mathcal{P}_b)^{w-j}, & \text{for odd } w, \\ 0.5\binom{w}{w/2}\mathcal{P}_b^{w/2}(1-\mathcal{P}_b)^{w/2} + \sum\limits_{j=w/2+1}^{w} \binom{w}{j} \mathcal{P}_b^j (1-\mathcal{P}_b)^{w-j}, & \text{for even } w \end{cases} \tag{26}$$

In (26), $\mathcal{P}_b$ is the bit error probability of the uncoded systems in an AWGN channel, which is given as $\mathcal{P}_{b(\text{DCO-VC})}$ and $\mathcal{P}_{b(\text{DCO-OFDM})}$ in (23) and (24), respectively.

V. System Performance over VLC Channels

In this section, the performance of DCO-OFDM and DCO-VC schemes is examined over the indoor VLC hybrid and diffuse links. The throughput performance of the two schemes is compared in uncoded and Coded-SD transmission modes. The Coded-HD mode is not considered here as the AWGN results show that SD detection is more spectrally efficient.

A. Performance over hybrid links

The investigation was carried out based on three different Rx locations in the considered room (see Fig. 4), leading to three different hybrid channels. These locations are referred to as A, B and C in this paper. The exact Rx co-ordinates for

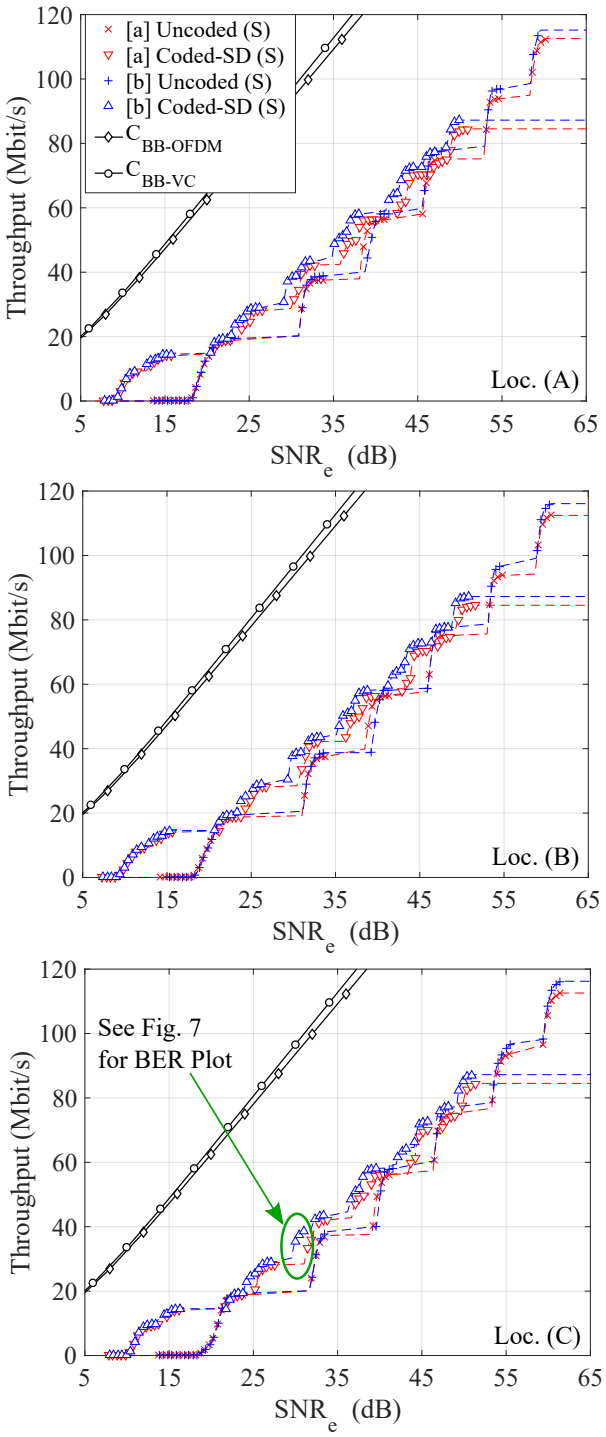

Fig. 6. Throughput of uncoded and coded [a] DCO-OFDM and [b] DCO-VC schemes over different hybrid links in considered indoor environment. The dashed curves are obtained by curve fitting from the simulation (S) results shown by markers.

each location can be found in Table II, where the *rms* delay spread (τ_{rms}) for each channel is given, as calculated by [47]:

$$\tau_{rms} = \sqrt{\bar{\tau^2} - \bar{\tau}^2}, \tag{27}$$

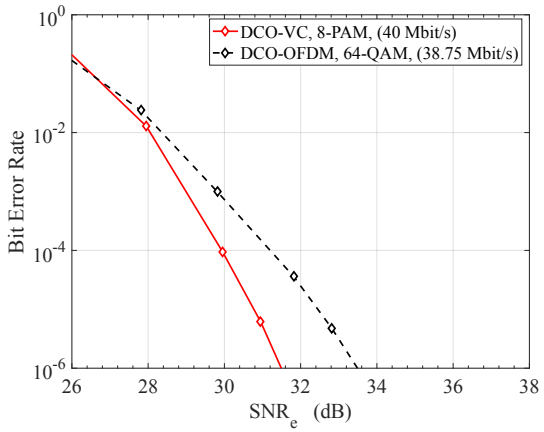

Fig. 7. BER of the Coded-SD based DCO-OFDM and DCO-VC systems over hybrid link at location C for a throughput of approximately 40 Mbit/s at BER = 10^{-6}.

TABLE II
THE CHANNEL τ_{rms} AND K VALUES AT DIFFERENT RX LOCATIONS WHILE THE TX IS LOCATED AT $(2.5, 2.5, 2.5)$, AT A SYMBOL RATE OF $R_s = 20$ MS/S.

Rx Location	**Coordinates (m) {x, y, z}**	τ_{rms} (ns)	K(dB)
A	$(2.5, 2.5, 0.85)$	0.340	23.80
B	$(1.5, 1.5, 0.85)$	0.867	14.22
C	$(0.5, 0.5, 0.85)$	3.408	0.00

where, $\bar{\tau} = \sum_{j=0}^{J-1} |h_j|^2 t_j \Big/ \sum_{j=0}^{J-1} |h_j|^2$ is the mean excess delay and $\bar{\tau^2} = \sum_{j=0}^{J-1} |h_j|^2 t_j^2 \Big/ \sum_{j=0}^{J-1} |h_j|^2$ is the mean square excess delay spread. Table II also shows the K-factor values for the hybrid VLC links, which can be computed from (13) and (14) as [38]:

$$K = (\eta/\zeta)^2 \tag{28}$$

The channel impulse response $h(t)$ in (12) was obtained based on the properties of the room in Fig. 4, the system parameters shown in Table I, and the reflectivity of the room ceiling, plaster wall, plastic wall and room floor for the blue colour channel (i.e. $\lambda \sim 450$ nm). The ρ value observed in [48] for the blue band is approximately 0.454, which was used to evaluate $h(t)$. Table II show that minimum dispersion will be experienced at the centre (Location A) of the room, where K is highest as η is much larger than ζ. As the Rx is moved towards location C, K decreases and τ_{rms} increases as ζ becomes comparable to η. This behaviour of hybrid links is also seen in [38], where it is shown that the hybrid link's optical powers and cut-off bandwidths decrease as a function of η and tend to be similar to those in diffuse links as the Rx moves from the room centre (where Tx is situated) towards the walls.

During the simulations, $N = 64$ sub-channels were used, to keep the sub-channel (or sub-block) bandwidth ($W_N = \frac{W}{N}$) much less than the channel coherence bandwidth ($W_C \approx \frac{0.2}{\tau_{rms}}$), i.e. $W_N << W_C$. A W of 20 MHz, and the τ_{rms} experienced in the diffuse link (sec. V-B), estimates that an N of 8 could be used to decrease the system complexity,

given W_N=0.1W_C [31]. On the other hand, an N of 64 provides good complexity compromise and has been used in many standard communications systems such as Wi-Fi. Additionally, to achieve high throughputs, VLC systems are expected to switch LEDs beyond their cut-off bandwidths, as well as micro-LEDs suitable for VLC with cut-off bandwidths $>$ 100 MHz have been produced [49]. This means $N > 8$ will be required, to achieve very high data throughput with W>>20 MHz. The value of μ was computed as μ=$\frac{\tau_{rms}}{T_s}$−1 [31], where T_s is the sample duration, which gave μ of 2 for the diffuse links. Therefore, μ=2, was used for all the investigations over the indoor VLC channels.

Fig. 6 shows a throughput comparison of the DCO-OFDM and DCO-VC systems in uncoded and Coded-SD transmission modes over the three Rx locations considered. These results show that for uncoded transmission modes, the DCO-OFDM and DCO-VC systems require almost the same levels of SNR_e to achieve a certain throughput in the hybrid indoor channels. However, in the Coded-SD transmissions, DCO-VC provides approximately up to 2 dB SNR_e gain when compared to DCO-OFDM for throughputs above 20 Mbit/s. This shows that for the higher modulation orders, the coded DCO-VC system is more power efficient than the coded DCO-OFDM. The BER comparison for the results region with significant performance difference between the two schemes is also shown in Fig. 7.

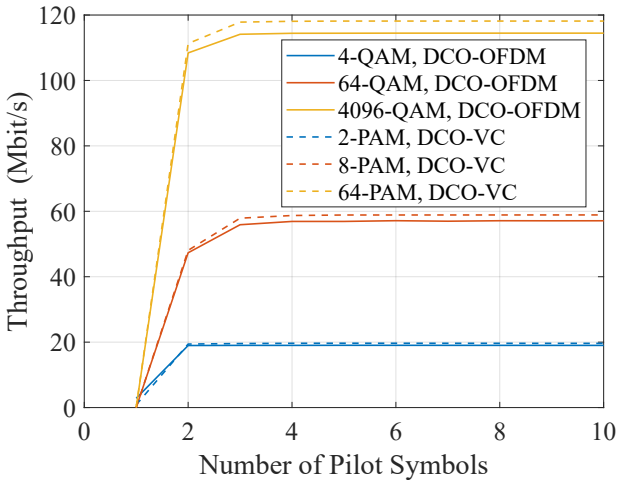

Fig. 8. Throughput of uncoded DCO-OFDM and DCO-OFDM in hybrid channel as a function of number of pilot symbol used for channel estimation. The receiver is at Loc. (C). Each simulation considers SNR_e level for a BER $\leq 10^{-6}$.

So far we have considered a scenario where perfect (noiseless) CSI is available at the transmitter and receiver side. However, the channel sounding process can be prone to noise itself. We therefore, must look into the impact of the noise in channel estimation on the achievable throughout, considering the number of pilot symbols used for channel estimation. We assume to estimate the channel coefficients according to the minimum mean square error [50]. Under the hypothesis of transmitting up to ten pilot symbols every second and that the SNR during the estimation phase is the same of the communication, we report the effect of noisy estimation on the

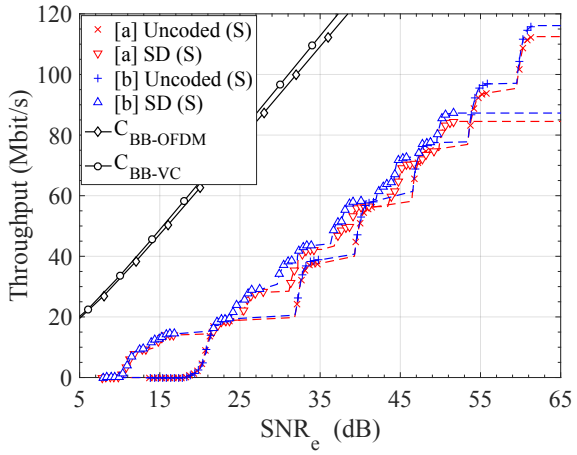

Fig. 9. Throughput of uncoded and Coded-SD [a] DCO-OFDM and [b] DCO-VC schemes over diffuse channel. The dashed curves are obtained by curve fitting from the simulation (S) results shown by markers.

throughput of both the DCO-VC and DCO-OFDM systems. The results are shown in Fig. 8, which consider a hybrid channel with receiver at Loc. (C) and an SNR_e sufficient to provide a BER $\leq 10^{-6}$. These results show that the DCO-OFDM and DCO-VC systems will require between 2 to 4 pilot symbols for obtaining a good CSI, depending on M.

B. Performance over diffuse link

1) Diffuse Links - Part I: In this section the performance of the considered uncoded and Coded-SD systems is examined over a diffuse (non-LOS) indoor link. In practical scenarios, the LOS in hybrid indoor links can be either blocked or may not be present due to the limited Rx FOV. In this case the VLC systems must rely upon the diffuse signals. The impulse response of diffuse indoor links has been verified through measurements in [38] and can be given as (29) [51][38], which is the same as (12) when η=0. It is shown in [38], that the optical power and the cut-off bandwidth of the channel in diffuse links are uniform across a room of the type considered and depends upon ρ and $\langle t \rangle$. Therefore, $h_{Dif}(t)$ is also uniform across the room. The τ_{rms} in this case can also be approximated from (16) as τ_{rms}=τ_c/2= − $\langle t \rangle$/2 ln(ρ) [52]. For the considered room (Fig. 4) and the ρ value used in the previous section, the τ_{rms} of a diffuse channel approximates to 5.7 ns, which is comparable to τ_{rms} of a hybrid link at location C.

$$h_{Dif}(t) = \frac{\zeta}{\tau_c} \exp\left(-\frac{t - \Delta t_{dif}}{\tau_c}\right) u(t - \Delta t_{dif}) \qquad (29)$$

Fig. 9 shows the throughput performance of the considered systems in uncoded and Coded-SD modes. During the simulations, N was kept equal to 64 in this case as well, satisfying W_N<<W_C and μ of 2 was sufficient to avoid ISI. The results for the diffuse channel are similar to those at location C in the hybrid links (Fig. 6). This shows that all the schemes are very effective at equalising the channel dispersion over the diffuse link too. Similar to the results seen in a hybrid channel, in the Coded-SD mode, the DCO-VC scheme provides up to 2

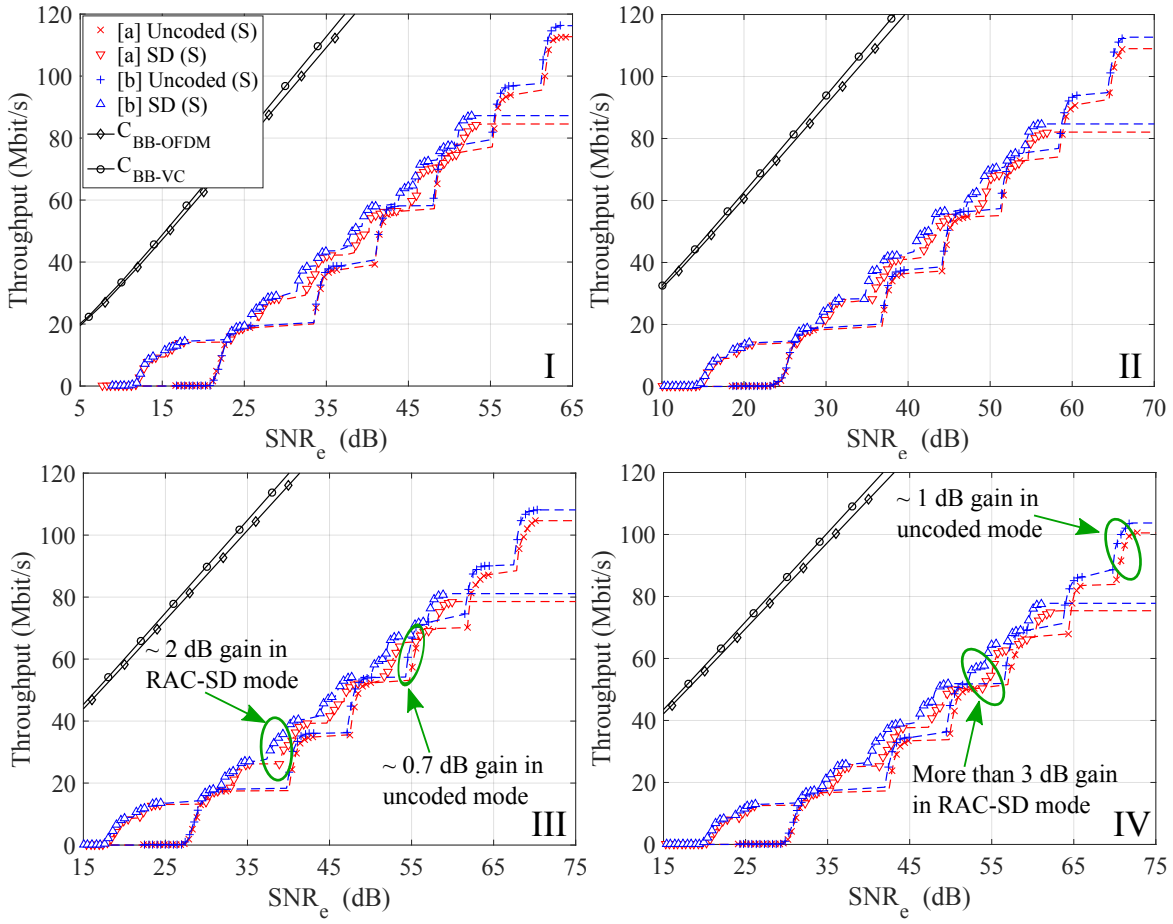

Fig. 10. Throughput of the uncoded and Coded-SD, [a] DCO-OFDM and [b] DCO-VC schemes over four diffuse links with different τ_{rms}: (I) 10ns, (II) 20ns, (III) 35ns and (IV) 50ns. The dashed curves are obtained by curve fitting from the simulation (S) results shown by markers.

dB SNR_e gain for the same throughput when compared to the DCO-OFDM in the diffuse channel.

2) Diffuse Links - Part-II: The previous sub-section shows that the maximum τ_{rms} experienced over the considered room (Fig. 4), with key system parameters shown in Table I, will be 5.7ns for a diffuse link. The τ_{rms}, as previously mentioned, is directly proportional to $\langle t \rangle$ given ρ is almost unity. Therefore, for a room of larger size the τ_c and hence τ_{rms} will be larger. In order to study the performance of the considered systems with higher temporal dispersion, four diffuse links each with τ_{rms} value of (I) 10ns, (II) 20ns, (III) 35ns and (IV) 50ns were used. In this case the diffuse CIR $h_{dif}(\tau)$ was obtained by directly setting the τ_c and τ_{rms} without defining the characteristics of the room.

The throughput performance of each system was evaluated through simulations over each diffuse link which is shown in Fig. 10. W was kept at 20 MHz and an N of 64 was used during the simulations. A μ of 2, 4, 7 and 10 was sufficient to avoid ISI over the diffuse links with τ_{rms} of 10ns, 20ns, 35ns and 50ns, respectively. The results show that the SNR_e requirements increase as the τ_{rms} increases and the throughput decreases due to increase in the prefix length.

The results in Fig. 10 show the same trends as the results in Fig. 9 and as the results in Fig. 6. However, it can be noticed from Fig. 10 that as the τ_{rms} increases, the power efficiency of the DCO-VC also increases. In the Coded-SD mode at τ_{rms} of 50ns, the DCO-VC scheme provides more than 3 dB SNR_e gain when compared to DCO-OFDM. Additionally, in the uncoded mode at τ_{rms} of 50ns, the DCO-VC scheme provides more than 1 dB SNR_e gain when compared to DCO-OFDM. This shows that a coded DCO-VC system can lead to large SNR gains in highly dispersive indoor VLC channels.

In addition to the SNR gains seen through the DCO-VC system over the DCO-OFDM for all the channels considered in this paper, it must be noted that for both the optical MCM schemes, the Coded-SD transmission mode can provide approximately up to 9 dB SNR_e gain in comparison to the uncoded transmission mode (see Fig. 6, Fig. 9 and Fig. 10). This shows that a BC coding based coded schemes will significantly enhance the overall throughput of the VLC systems. The considered BC code has been widely used in current communication systems, such as Wi-Fi and Wi-MAX, hence the hardware implementation will not impose any significant challenge.

C. Computational complexity

The computational complexities of the DVO-VC and DCO-OFDM schemes is an important aspect of the performance

comparison. The DCO-OFDM (without precoding) requires $\frac{N}{2}log_2N$ complex multiplications and $Nlog_2N$ complex additions for the IFFT at the transmitter [53]. Similarly, at the receiver, the DCO-OFDM requires $\frac{N}{2}log_2N$ complex multiplications and $Nlog_2N$ complex additions for the FFT. Furthermore, the DCO-OFDM requires N complex multiplications at the receiver for channel equalisation. In comparison to this, the DCO-VC requires N^2 real multiplications and $N(N-1)$ real additions at the transmitter and at the receiver each. Considering an N of 8 (64), the DCO-OFDM requires 88 (1280) additions and 80 (1024) multiplications at the transmitter and receiver each. On the other hand, the DCO-VC requires 56 (4032) additions and 64 (4096) multiplications at the receiver and transmitter each. Therefore, the computational complexity of DCO-VC is lower than DCO-OFDM for small N only. Therefore, the SNR gain achived by DCO-VC must be carefully traded-off with the additional computational overload required for higher N, which may be required for highly non-linear communication channels. In the case of precoded DCO-OFDM, a further N^2 complex multiplications must be considered at the transmitter.

VI. Conclusion

A new multi-channel modulation scheme, DCO-VC, has been proposed for quasi-static optical wireless links, which uses the channel state information at the transmitter and receiver to partition the channel into orthogonal sub-channels. The throughput performance of the DCO-VC scheme has been evaluated over various LOS and NLOS indoor VLC channels and compared against the well-known DCO-OFDM system. The results show that DCO-VC outperforms the DCO-OFDM scheme by achieving up to 2 dB and 3 dB SNR gains in the hybrid and diffuse channels, respectively. Moreover, the results show that as the dispersion in the VLC channel increases the SNR gains with the proposed DCO-VC system increase further. The performance evaluation results also show that the well-known BC codes with puncturing technique could provide up to 9 dB SNR gain for the DCO-OFDM and DCO-VC systems when compared to their performance in uncoded transmission modes.

Potential future investigations could include use of channel adaptive modulation with MMSE equalisation to further study the system throughput performance improvements. The opportunity of decomposing the electrical channel along with the optical channel through vector coding also exists, especially considering transmission rates exceeding the -3 dB bandwidth.

Acknowledgment

The authors would like to thank Professor John M Cioffi of Stanford University, for his invaluable advice in understanding optimal channel partitioning vectors.

References

[1] "IEEE Standard for Local and Metropolitan Area Networks–Part 15.7: Short-Range Wireless Optical Communication Using Visible Light," *IEEE Std 802.15.7-2011*, pp. 1 –309, 6 2011.

[2] IEEE 802.15 WPANTM. 15.7 Revision: Short-Range Optical Wireless Communications Task Group (TG 7r1) (Accessed July 2015). [Online]. Available: http://www.ieee802.org/15/pub/IEEE%20802_15%20WPAN%2015_7%20Revision1%20Task%20Group.htm

[3] L. Zeng, D. O'Brien, H. Le-Minh, K. Lee, D. Jung, and Y. Oh, "Improvement of date rate by using equalization in an indoor visible light communication system," in *ICCSC 2008*, May 2008, pp. 678–682.

[4] D. O'Brien, L. Zeng, H. Le-Minh, G. Faulkner, J. Walewski, and S. Randel, "Visible light communications: Challenges and possibilities," in *IEEE PIMRC*, 2008, pp. 1–5.

[5] A. T. Hussein and J. M. Elmirghani, "Mobile multi-gigabit visible light communication system in realistic indoor environment," *Journal of Lightwave Technology*, vol. 33, no. 15, pp. 3293–3307, 2015.

[6] D. Tsonev, S. Videv, and H. Haas, "Towards a 100 gb/s visible light wireless access network," *Optics express*, vol. 23, no. 2, pp. 1627–1637, 2015.

[7] L. Zeng, D. O'Brien, H. Minh, G. Faulkner, K. Lee, D. Jung, Y. Oh, and E. T. Won, "High data rate multiple input multiple output (mimo) optical wireless communications using white led lighting," *IEEE J. Sel. Areas Commun.*, vol. 27, no. 9, pp. 1654–1662, 2009.

[8] F. Dong, R. Singh, and D. O'Brien, "Adaptive mimo-vlc system for high data rate communications," in *2020 IEEE Globecom Workshops (GC Wkshps*, 2020, pp. 1–6.

[9] R. Singh, T. O'Farrell, and J. P. David, "An enhanced color shift keying modulation scheme for high-speed wireless visible light communications," *Journal of Lightwave Technology*, vol. 32, no. 14, pp. 2582–2592, 2014.

[10] R. Singh, S. Pergoloni, T. O'Farrell, G. Scarano, J. David, and M. Biagi, "White light constrained multi-primary modulation for visible light communication," in *2017 IEEE Globecom Workshops (GC Wkshps)*. IEEE, 2017, pp. 1–6.

[11] T.-C. Bui, R. Singh, T. O'Farrell, G. Scarano, J. P. David, and M. Biagi, "Optimized multi-primary modulation for visible light communication," *Journal of Lightwave Technology*, vol. 40, no. 22, pp. 7254–7264, 2022.

[12] M. B. Rahaim and T. D. Little, "Toward practical integration of dual-use vlc within 5g networks," *IEEE Wireless Communications*, vol. 22, no. 4, pp. 97–103, 2015.

[13] X. Wu, D. C. O'Brien, X. Deng, and J.-P. M. Linnartz, "Smart handover for hybrid lifi and wifi networks," *IEEE Transactions on Wireless Communications*, vol. 19, no. 12, pp. 8211–8219, 2020.

[14] R. Singh, T. O'Farrell, and J. P. David, "Performance evaluation of ieee 802.15.7 csk physical layer," in *IEEE Globecom Workshops*, Dec 2013, pp. 1064–1069.

[15] R. Singh, T. O'Farrell, and J. David, "Analysis of forward error correction schemes for colour shift keying modulation," in *IEEE PIMRC*, Hong Kong, P.R. China, Aug. 2015.

[16] Z. Ahmed, R. Singh, W. Ali, G. Faulkner, D. O'Brien, and S. Collins, "A sipm-based vlc receiver for gigabit communication using ook modulation," *IEEE Photonics Technology Letters*, vol. 32, no. 6, pp. 317–320, 2020.

[17] A. Surampudi, R. Singh, G. Faulkner, D. O'Brien, and S. Collins, "Raised cosine pulse shaping for pre-equalized optical wireless links," *IEEE Photonics Technology Letters*, pp. 1–1, 2021.

[18] A. Surampudi, R. Singh, A. Riaz, W. Ali, G. Faulkner, D. O'Brien, and S. Collins, "A digital pre-equalizer for optical wireless links," *Journal of Lightwave Technology*, vol. 40, no. 4, pp. 961–967, 2021.

[19] O. González, R. Pérez-Jiménez, S. Rodriguez, J. Rabadán, and A. Ayala, "Ofdm over indoor wireless optical channel," *IEE Proceedings-Optoelectronics*, vol. 152, no. 4, pp. 199–204, 2005.

[20] J. B. Carruthers and J. M. Kahn, "Multiple-subcarrier modulation for nondirected wireless infrared communication," *IEEE Journal on Selected Areas in Communications*, vol. 14, no. 3, pp. 538–546, 1996.

[21] J. Armstrong and B. J. Schmidt, "Comparison of asymmetrically clipped optical ofdm and dc-biased optical ofdm in awgn," *IEEE communications letters*, vol. 12, no. 5, pp. 343–345, 2008.

[22] D. Tsonev, S. Sinanovic, and H. Haas, "Novel unipolar orthogonal frequency division multiplexing (u-ofdm) for optical wireless," in *IEEE VTC Spring, 2012*, May 2012, pp. 1–5.

[23] N. Fernando, Y. Hong, and E. Viterbo, "Flip-ofdm for unipolar communication systems," *IEEE Transactions on Communications*, vol. 60, no. 12, pp. 3726–3733, December.

[24] J. Grubor, S. Randel, K.-D. Langer, and J. Walewski, "Broadband information broadcasting using led-based interior lighting," *Journal of Lightwave Technology*, vol. 26, no. 24, pp. 3883–3892, Dec 2008.

[25] M. Wolf and M. Haardt, "Comparison of ofdm and frequency domain equalization for dispersive optical channels with direct detection," in *ICTON, 2012*. IEEE, 2012, pp. 1–7.

[26] L. Wu, Z. Zhang, J. Dang, and H. Liu, "Adaptive modulation schemes for visible light communications," *Journal of Lightwave Technology*, vol. 33, no. 1, pp. 117–125, 2015.

[27] R. Singh, "Physical layer techniques for indoor wireless visible light communications," Ph.D. dissertation, University of Sheffield, 2015.

[28] S. Kasturia, J. T. Aslanis, and J. M. Cioffi, "Vector coding for partial response channels," *IEEE transactions on Information Theory*, vol. 36, no. 4, pp. 741–762, 1990.

[29] J. M. Cioffi, "Chappter 4: Multi-channel modulation." [Online]. Available: http://www.stanford.edu/group/cioffi/ee379c/

[30] A. Azhar and D. O'Brien, "Experimental comparisons of optical ofdm approaches in visible light communications," in *GLOBECOM Workshops (GC Wkshps), 2013 IEEE*, Dec 2013.

[31] A. Goldsmith, *Wireless Communications*. Cambridge Univerity Press, 2005.

[32] "Ieee standard for air interface for broadband wireless access systems," *IEEE Std 802.16-2012 (Revision of IEEE Std 802.16-2009)*, pp. 1–2542, Aug 2012.

[33] Q. Wang, Q. Xie, Z. Wang, S. Chen, and L. Hanzo, "A universal low-complexity symbol-to-bit soft demapper," *IEEE Transactions on Vehicular Technology*, vol. 63, no. 1, pp. 119–130, 2014.

[34] R. van Nee and R. Prasad, *OFDM for Wireless Multimedia Communications*. Artech House, Boston, London, 2000.

[35] S. D. Dissanayake and J. Armstrong, "Comparison of aco-ofdm, dco-ofdm and ado-ofdm in im/dd systems," *Journal of lightwave technology*, vol. 31, no. 7, pp. 1063–1072, 2013.

[36] T. Komine and M. Nakagawa, "Fundamental analysis for visible-light communication system using led lights," *IEEE Transactions on Consumer Electronics*, vol. 50, no. 1, pp. 100–107, 2004.

[37] M. Uysal, F. Miramirkhani, O. Narmanlioglu, T. Baykas, and E. Panayirci, "Ieee 802.15. 7r1 reference channel models for visible light communications," *IEEE Communications Magazine*, vol. 55, no. 1, pp. 212–217, 2017.

[38] V. Jungnickel, V. Pohl, S. Nonnig, and C. von Helmolt, "A physical model of the wireless infrared communication channel," *IEEE JSAC*, vol. 20, no. 3, pp. 631–640, Apr 2002.

[39] Thorlabs, "FB450-40 Bandpass Filter [Online]. Available: http://www.thorlabs.de/thorproduct.cfm?partnumber=FB450-40," 2014.

[40] First Sensor, "PC10-6b PIN PD [Online]. Available: http://www.first-sensor.com/en/datasheet/501229," 2014.

[41] K. Cho and D. Yoon, "On the general ber expression of one-and two-dimensional amplitude modulations," *IEEE Transactions on Communications*, vol. 50, no. 7, pp. 1074–1080, 2002.

[42] John G. Proakis and Masoud Salehi, *Digital Communications*, 5th ed. McGraw-Hill, 2008.

[43] Shu Lin and Daniel J. Costello, Jr., *Error Control Coding: Fundamentals and Applications*. Prentice-Hall, Inc., 1983.

[44] J. Conan, "The weight spectra of some short low-rate convolutional codes," *Comms., IEEE Trans. on*, vol. 32, no. 9, pp. 1050–1053, Sep 1984.

[45] Jeff Foerster and John Liebetreu. (2000, June) FEC Performance of Concatenated Reed-Solomon and Convolutional Coding with Interleaving. [Online]. Available: http://www.ieee802.org/16/tg1/phy/contrib/802161pc-00_33.pdf

[46] S. Rajbhandari, Z. Ghassemlooy, and N. Aldibbiat, "Performance of convolutional coded dual header pulse interval modulation in infrared links," in *6th PGNET, UK*, 2006, pp. 227–231.

[47] T. O'Farrell, "Statistical fading models: Narrowband and wideband fading." [Online]. Available: http://hercules.shef.ac.uk/eee/teach/resources/eee6431/Lecture_3.pdf

[48] K. Lee, H. Park, and J. Barry, "Indoor channel characteristics for visible light communications," *IEEE Commun. Lett.*, vol. 15, no. 2, pp. 217–219, February 2011.

[49] J. J. McKendry, D. Massoubre, S. Zhang, B. R. Rae, R. P. Green, E. Gu, R. K. Henderson, A. Kelly, and M. D. Dawson, "Visible-light communications using a cmos-controlled micro-light-emitting-diode array," *Journal of Lightw. Technol.*, vol. 30, no. 1, pp. 61–67, 2012.

[50] H. V. Poor, *An introduction to signal detection and estimation*. Springer Science & Business Media, 1998.

[51] V. Pohl, V. Jungnickel, and C. Von Helmolt, "Integrating-sphere diffuser for wireless infrared communication," *IEE Proceedings-Optoelectronics*, vol. 147, no. 4, pp. 281–285, 2000.

[52] J. B. Carruthers and J. M. Kahn, "Modeling of nondirected wireless infrared channels," *IEEE Trans. Commun.*, vol. 45, no. 10, pp. 1260–1268, 1997.

[53] S.-H. Wang, C.-P. Li, K.-C. Lee, and H.-J. Su, "A novel low-complexity precoded ofdm system with reduced papr," *IEEE Transactions on Signal Processing*, vol. 63, no. 6, pp. 1366–1376, 2015.